Palmprint Feature Extraction Using 2-D Gabor Filters

Wai Kin Kong, David Zhang and Wenxin Li

Biometrics Research Centre
Department of Computing
The Hong Kong Polytechnic University
Kowloon, Hong Kong

Corresponding author:

Prof. David Zhang
Biometrics Research Centre
Department of Computing
The Hong Kong Polytechnic University
Hung Hom, Kowloon, Hong Kong
Phone: (852) 2766-7271
Fax: (852) 2774-0842
E-mail: csdzhang@comp.polyu.edu.hk

Abstract — Biometric identification is an emerging technology that can solve security problems in our networked society. A few years ago, a new branch of biometric technology, palmprint authentication, was proposed [1] whereby lines and points are extracted from palms for personal identification. In this paper, we consider the palmprint as a piece of texture and apply texture-based feature extraction techniques to palmprint authentication. A 2-D Gabor filter is used to obtain texture information and two palmprint images are compared in terms of their hamming distance. The experimental results illustrate the effectiveness of our method.

Index Terms — Palmprint, Gabor filter, biometrics, feature extraction, texture analysis

1. Introduction

Computer-based personal identification, also known as biometric computing, which attempts to recognize a person by his/her body or behavioral characteristics, has more than 30 years of history. The first commercial system, called *Identimat,* which measured the shape of the hand and the length of fingers, was developed in the 1970s. At the same time, fingerprint-based automatic checking systems were widely used in law enforcement. Because of the rapid development of hardware, including computation speed and capture devices, iris, retina, face, voice, signature and DNA have joined the biometric family [2-3,24].

Fingerprint identification has drawn considerable attention over the last 25 years. However, some people do not have clear fingerprints because of their physical work or problematic skin. Iris and retina recognition provide very high accuracy but suffer from high costs of input devices or intrusion into users. Recently, many researchers have focused on face and voice verification systems; nevertheless, their performance is still far from satisfactory [20]. The accuracy and uniqueness of 3-D hand geometry are still open questions

[2,4,20]. Compared with the other physical characteristics, palmprint authentication has several advantages: 1) low-resolution imaging; 2) low intrusiveness; 3) stable line features and 4) high user acceptance.

Palmprint authentication can be divided into two categories, *on-line* and *off-line*. Fig. 1 (a) and (b) show an on-line palmprint image and an off-line palmprint image, respectively. Research on off-line palmprint authentication has been the main focus in the past few years [1,5,22-23], where all palmprint samples are inked on paper, then transmitted into a computer through a digital scanner. Due to the relative high-resolution off-line palmprint images (up to 500 dpi), some techniques applied to fingerprint images could be useful for off-line palmprint authentication, where lines, datum points and singular points can be extracted [1,5]. For on-line palmprint authentication, the samples are directly obtained by a palmprint scanner [25-26]. Recently, a CCD based palmprint capture device has been developed by us [25]. Fig. 2(a) shows a palmprint image captured by our palmprint scanner and Fig. 2(b) shows the outlook of the device. Note that a low-resolution technique (75 dpi) is adopted to reduce the image size, which is comparable with fingerprint images even though a palm is much larger than a fingerprint. It is evident that on-line identification is more important for many real-time applications, so that it draws our attention to investigate.

Our on-line palmprint verification system contains five modules, palmprint acquisition, preprocessing, feature extraction, matching and storage. Fig. 3 gives a block diagram to describe the relationship between the five modules. The five modules are described below:

1) Palmprint Acquisition: A palmrpint image is captured by our palmprint scanner and then the AC signal is converted into a digital signal, which is transmitted to a computer for further processing.

2) Preprocessing: A coordinate system is set up on basis of the boundaries of fingers so as to extract a central part of a palmprint for feature extraction.

3) Textured Feature Extraction: We apply a 2-D Gabor filter to extract textural information from the central part.

4) Matching: A distance measure is used to measure the similarity of two palmprints.

5) Database: It is used to store the templates obtained from the enrollment phase.

Our palmprint authentication system can operate in two modes, enrollment and verification. In the enrollment mode, a user is to provide several palmprint samples to the system. The samples are captured by our palmprint scanner and passes through preprocessing and feature extraction to produce the templates stored in a given database. In the verification mode, the user is asked to provide his/her user ID and his/her palmprint sample. Then the palmprint sample passes through preprocessing and feature extraction. The extracted features are compared with templates in the database belonging to the same user ID.

In this paper, we attempt to apply a textural extraction method to palmprint images for personal authentication. The remaining sections are organized as follows: preprocessing steps are mentioned in Section 2. Palmprint feature extraction by texture analysis is explained in Section 3. Experimental results are given in Section 4. Finally, Section 5 summaries the main results of this paper.

2. Palmprint Image Preprocessing

Before feature extraction, it is necessary to obtain a sub-image from the captured palmprint image and to eliminate the variations caused by rotation and translation. The five main steps of palmprint image preprocessing are as follows (see Fig. 4).

Step 1: Apply a low-pass filter to the original image. Then use a threshold, T_p, to convert this original image into a binary image as shown in Fig. 4(b). Mathematically, this transformation can be represented as

$$B(x, y)=1 \text{ if } O(x, y) * L(x, y) \geq T_p, \quad (1)$$

$$B(x, y)=0 \text{ if } O(x, y) * L(x, y) < T_p, \quad (2)$$

where $B(x,y)$ and $O(x,y)$ are the binary image and the original image, respectively; $L(x,y)$ is a lowpass filter, such as Gaussian, and "$*$" represents an operator of convolution.

Step 2: Extract the boundaries of the holes, (F_ix_j, F_iy_j), (i=1,2), between fingers using a boundary-tracking algorithm. The start points, (Sx_i, Sy_i), and end points, (Ex_i, Ey_i), of the holes are then marked in the process (see Fig. 4(c)).

Step 3: Compute the center of gravity, (Cx_i, Cy_i), of each hole with the following equations:

$$Cx_i = \frac{\sum_{j=1}^{M(i)} F_i x_j}{M(i)}, \quad (3)$$

$$Cy_i = \frac{\sum_{j=1}^{M(i)} F_i y_j}{M(i)}, \quad (4)$$

where $M(i)$ represents the number of boundary points in the hole, i. Then construct a line that passes through (Cx_i, Cy_i) and the midpoint of (Sx_i, Sy_i) and (Ex_i, Ey_i). The line equation is defined as

$$y = x\frac{(Cy_i - My_i)}{(Cx_i - Mx_i)} + \frac{My_i Cx_i - Mx_i Cy_i}{Cx_i - Mx_i}, \quad (5)$$

where (Mx_i, My_i) is the midpoint of (Sx_i, Sy_i) and (Ex_i, Ey_i). Based on these lines, two key points, (k_1, k_2), can easily be detected (see Fig. 4(d)).

Step 4: Line up k_1 and k_2 to get the Y-axis of the palmprint coordinate system and make a line through their mid point which is perpendicular to the Y-axis, to determine the origin of the coordinate system (see Fig. 4(e)). This coordinate system can align different palmprint images.

Step 5: Extract a sub-image with the fixed size on the basis of coordinate system, which is located at the certain part of the palmprint for feature extraction (see Fig. 4(f)).

3. Palmprint Feature Extraction By Texture Analysis

This section defines our palmprint feature extraction method, which includes filtering and matching. The motivation for using a Gabor filter in our palmprint research is first discussed.

3.1 Gabor Function

Gabor filter, Gabor filter bank, Gabor transform and Gabor wavelet are widely applied to image processing, computer vision and pattern recognition. This function can provide accurate time-frequency location governed by the "Uncertainty Principle" [6-7]. A circular 2-D Gabor filter in the spatial domain has the following general form [8-9],

$$G(x, y, q, u, s) = \frac{1}{2ps^2}\exp\left\{-\frac{x^2 + y^2}{2s^2}\right\}\exp\{2pi(ux\cos q + uy\sin q)\}, \quad (6)$$

where $i = \sqrt{-1}$; u is the frequency of the sinusoidal wave; q controls the orientation of the function and s is the standard deviation of the Gaussian envelope. Such Gabor filters have

been widely used in various applications [10-19]. In addition to accurate time-frequency location, they also provide robustness against varying brightness and contrast of images. Furthermore, the filters can model the receptive fields of a simple cell in the primary visual cortex. Based on these properties, in this paper, we try to apply a Gabor filter to palmprint authentication.

3.2 Filtering and Feature Extraction

Generally, principal lines and wrinkles can be observed from our captured palmprint images (see Fig. 1(a)). Some algorithms such as the stack filter [21] can obtain the principal lines. However, these lines do not contribute adequately to high accuracy because of their similarity amongst different palms. Fig. 5 shows six palmprint images with similar principal lines. Thus, wrinkles play an important role in palmprint authentication but accurately extracting them is still a difficult task. This motivates us to apply texture analysis to palmprint authentication.

In fact, a Gabor function, $G(x, y, q, u, s)$ with a special set of parameters (s, q, u), is transformed into a discrete Gabor filter, $G[x, y, q, u, s]$. The parameters are chosen from 12 sets of parameters listed in Table 1 based on the experimental results in the next section. In order to provide more robustness to brightness, the Gabor filter is turned to zero DC (direct current) with the application of the following formula:

$$\tilde{G}[x, y, q, u, s] = G[x, y, q, u, s] - \frac{\sum_{i=-n}^{n} \sum_{j=-n}^{n} G[i, j, q, u, s]}{(2n+1)^2}, \qquad (7)$$

where $(2n+1)^2$ is the size of the filter. In fact, the imaginary part of the Gabor filter automatically has zero DC because of odd symmetry. This adjusted Gabor filter will convolute with a sub-image defined in Section 2. The sample point in the filtered image is coded to two bits, (b_r, b_i), by the following inequalities,

$$b_r=1 \text{ if } \mathrm{Re}[\tilde{G}[x, y, q, u, s] * I] \geq 0, \quad (8)$$

$$b_r=0 \text{ if } \mathrm{Re}[\tilde{G}[x, y, q, u, s] * I] < 0, \quad (9)$$

$$b_i=1 \text{ if } \mathrm{Im}[\tilde{G}[x, y, q, u, s] * I] \geq 0, \quad (10)$$

$$b_i=0 \text{ if } \mathrm{Im}[\tilde{G}[x, y, q, u, s] * I] < 0, \quad (11)$$

where I is the sub-image of a palmprint. Using this coding method, only the phase information in palmprint images is stored in the feature vector. The size of the feature is 256 bytes. Fig. 6 shows the features generated by the 12 filters listed in Table 1. This texture feature extraction method has been applied to iris recognition [13].

3.3 Palmprint Matching

In order to describe clearly the matching process, each feature vector is considered as two 2-D feature matrices, real and imaginary. Palmprint matching is based on a normalized hamming distance. Let P and Q be two palmprint feature matrices. The normalized hamming distance can be defined as,

$$D_o = \frac{\sum_{i=1}^{N}\sum_{j=1}^{N}\left(P_R(i, j) \otimes Q_R(i, j) + P_I(i, j) \otimes Q_I(i, j)\right)}{2N^2}, \quad (12)$$

where P_R (Q_R) and P_I (Q_I) are the real part and the imaginary part of P (Q), respectively; the Boolean operator, "$\otimes$", is equal to zero if and only if the two bits, $P_{R(I)}(i,j)$ and $Q_{R(I)}(i,j)$ are equal and the size of the feature matrices is $N \times N$. It is noted that D_o is between 1 and 0. The hamming distance for perfect matching is zero. In order to provide translation invariance matching, Eq. (12) can be improved as

$$D_{\min} = \min_{|s|<S, |t|<T} \frac{\sum_{i=\max(1,1+s)}^{\min(N,N+s)}\sum_{j=\max(1,1+t)}^{\min(N,N+t)}\left(P_R(i+s, j+t) \otimes Q_R(i, j) + P_I(i+s, j+t) \otimes Q_I(i, j)\right)}{2H(s)H(t)}, \quad (13)$$

where *S=2* and *T=2* control the range of horizontal and vertical translation of a feature in the matching process, respectively and

$$H(s) = \min(N,\ N+s) - \max(1,\ 1+s)\,. \tag{14}$$

The hamming distance, D_{min}, can support translation matching; nevertheless, because of unstable preprocessing, it is not a rotational invariant matching. Therefore, in enrollment mode, the coordinate system is rotated by a few degrees and then the sub-images are extracted for feature extraction. Finally, combining the effect of preprocessing and rotated features, Eq. (13) can provide both approximately rotational and translation invariance matching.

4. Experimental Results

4.1 Palmprint Database

In the following experiments, a palmprint database contains 4,647 palmprint images collected from 120 individuals by using our palmprint scanner. 43 of them are female, 111 of them are less than 30 years old and 2 of them are more than 50 years old. Each of them is asked to provide about 10 images for their left palm and 10 images for their right palm in each of two occasions. In total, each subject provides about 40 images. The average time difference of the first and second occasions is 81 days. The maximum and minimum are 4 and 162 days, respectively. Originally, the collected images have two sizes, 384×284 and 768×568. The large images are resized to 384×284; consequently, the size of all the test images in the following experiments is 384×284 with 75dpi resolution. The central parts of each image extracted with size 128 by 128 are named DBI. The preprocessed images in DBI resized to 64 by 64 are named DBII. The DBII is used to test the possibility of using lower-resolution palmprint images for personal identification. Fig. 7 shows nine typical images from our databases.

4.2 Verification Tests

To obtain better parameters for our system, 12 different sets of parameters listed in Table 1 are used to test the method. The first four filters are named as Level 1 filters since they are different in the parameter, q. Similarly, the other filters are named as Level 2 and Level 3. Each of the images in DBI (DBII) is matched with all other palmprint images in the same database. A matching is counted as a correct matching if two palmprint images are collected from the same palm; otherwise it is an incorrect matching. The total number of matchings for one verification test is 10,794,981. 43,660 of them are correct matchings and rest of them are incorrect matchings. In total, 24 verification tests are carried out for testing the 12 sets of parameters on the two databases. The performance of different parameters on the two databases is presented by Receiver Operating Characteristic (ROC) curves, which are a plot of genuine acceptance rate against false acceptance rate for all possible operating points. Figs. 8(a), 8(b) and 8(c) (8(d), 8(e) and 8(f)) show the ROC curves for DBI (DBII) generated by Levels 1, 2, 3 filters, respectively. According to the ROC curves, Level 3 filters are better than Levels 1 and 2 filters for DBI. According to Fig. 8(c), Filters 9, 10 and 11 provide similar performance when the false acceptance rate is greater than 10^{-2}. For false acceptance rates smaller than 10^{-2}, Filters 9 and 11 are better than Filter 10. For DBII, Level 1 filters are better than Level 2 and 3 filters. In fact, Filter 2 is the best for DBII. Although using very low-resolution images as DBII's images cannot provide very good performance, it still gives us an insight into using very low-resolution palmprint images for personal identification.

5. Conclusions

This paper reports a textured-based feature extraction method using low-resolution palmprint images for personal authentication. A palmprint is considered as a texture image, so an

adjusted Gabor filter is employed to capture the texture information on palmprints. Based on our tests, Filter 11 is the best of twelve filters in terms of accuracy. Combined with the effects of preprocessing and rotated preprocessed images, our matching process is translation and rotational invariance. Experimental results illustrate the effectiveness of the method.

Acknowledgments

The work is partially supported by the UGC (CRC) fund from Hong Kong Government and the central fund from The Hong Kong Polytechnic University.

References

[1] D. Zhang and W. Shu, "Two novel characteristics in palmprint verification: datum point invariance and line feature matching", *Pattern Recognition*, vol. 32, no. 4, pp. 691-702, 1999.

[2] A. Jain, R. Bolle and S. Pankanti (eds.), *Biometrics: Personal Identification in Networked Society*, Kluwer Academic Publishers, 1999.

[3] D. Zhang, *Automated Biometrics – Technologies and Systems*, Kluwer Academic Publishers, 2000.

[4] R. Sanchez, C. Sanchez-Avila and A. Gonzalez-Marcos, "Biometric identification through geometry measurements", *IEEE Transactions on Pattern Analysis and Machine Intelligence*, vol. 22, no. 10, pp. 1,168-1,171, 2000.

[5] W. Shu and D. Zhang, "Automated personal identification by palmprint", *Optical Engineering*, vol. 37 no. 8, pp.2,659-2,362, 1998.

[6] D. Gabor, "Theory of communications," *J. IEE*, vol. 93, pp. 429-457, 1946.

[7] C.K. Chui, *An Introduction to Wavelets*, Academic Press, Boston, 1992

[8] J.G. Daugman, "Two-dimensional spectral analysis of cortical receptive field profiles", *Vision Research*, vol. 20, pp. 847-856, 1980.

[9] J. Daugman, "Uncertainty relation for resolution in space, spatial frequency and orientation optimized by two-dimensional visual cortical filters", *Journal of the Optical Society of America A*, vol. 2, pp. 1,160-1,169, 1985.

[10] A. Jain and G. Healey, "A multiscale representation including opponent color features for texture recognition", *IEEE Transactions on Image Processing*, vol. 7, no. 1, pp. 124-128, 1998.

[11] D. Dunn and W.E. Higgins, "Optimal Gabor filters for texture segmentation", *IEEE Transactions on Image Processing*, vol. 4, no. 4, pp. 947-964, 1995.

[12] A.C. Bovik, M. Clark and W.S. Geisler, "Multichannel texture analysis using localized spatial filters", *IEEE Transactions on Pattern Analysis and Machine Intelligence*, vol. 12, no. 1, pp. 55-73, 1990.

[13] J. Daugman, "High confidence visual recognition of persons by a test of statistical independence", *IEEE Transactions on Pattern Analysis and Machine Intelligence*, vol. 15, no. 11, pp. 1,148-1,161, 1993.

[14] A.K. Jain, S. Prabhakar, L. Hong and S. Pankanti, "Filterbank-based fingerprint matching", *IEEE Transactions on Image Processing*, vol. 9, no. 5, pp. 846-859, 2000.

[15] L. Hong, Y. Wan and A. Jain, "Fingerprint image enhancement algorithm and performance evaluation", *IEEE Transactions on Pattern Analysis and Machine Intelligence*, vol. 20, no. 8, pp. 777-789, 1998.

[16] C.J. Lee and S.D. Wang. "Fingerprint feature extraction using Gabor filters", *Electronic Letters*, vol. 35, no. 4, pp. 288-290, 1999.

[17] M.J. Lyons, J. Budynek and S. Akamatsu, "Automatic classification of single facial images", *IEEE Transactions on Pattern Analysis and Machine Intelligence*, vol. 21, no. 12, pp. 1,357-1,362, 1999.

[18] B. Duc, S. Fischer and J. Bigun, "Face authentication with Gabor information on deformable graphs", *IEEE Transactions on Image Processing*, vol. 8, no. 4, pp. 504-516, 1999.

[19] Y. Adini, Y. Moses and S. Ullman, "Face recognition: The problem of compensation for changes in illumination direction", *IEEE Transactions on Pattern Analysis and Machine Intelligence*, vol. 19, no. 7, pp. 721-732, 1997.

[20] S. Pankanti, R.M. Bolle and A. Jain, "Biometrics: The Future of Identification", *IEEE Computer*, vol. 33, no. 2, pp. 46-49, 2000.

[21] P.S. Wu and M. Li. "Pyramid edge detection based on stack filter", *Pattern Recognition Letters*, vol. 18, no. 4, pp. 239-248, 1997.

[22] J. You, W. Li and D. Zhang, "Hierarchical palmprint identification via multiple feature extraction", *Pattern Recognition*, vol. 35, no. 4, pp. 847-859, 2002.

[23] N. Duta, A.K. Jain, and K.V. Mardia, "Matching of Palmprint", *Pattern Recognition Letters*, vol. 23, no. 4, pp. 477-485, 2001.

[24] D. Zhang (ed.), *Biometric Resolutions for Authentication in an e-World*, Kluwer Academic Publishers, 2002.

[25] D. Zhang, W.K. Kong, J. You and M. Wong, "On-line palmprint identification", To be appear in *IEEE Transactions on Pattern Recognition and Machine Intelligence*.

[26] C.C. Han, H.L. Cheng, K.C. Fan and C.L. Lin, "Personal authentication using palmprint features", *Pattern Recognition*, Special Issue: Biometrics, vol. 36, no 2, pp. 371-381, 2003.

Figures:

Tables:

Figures:

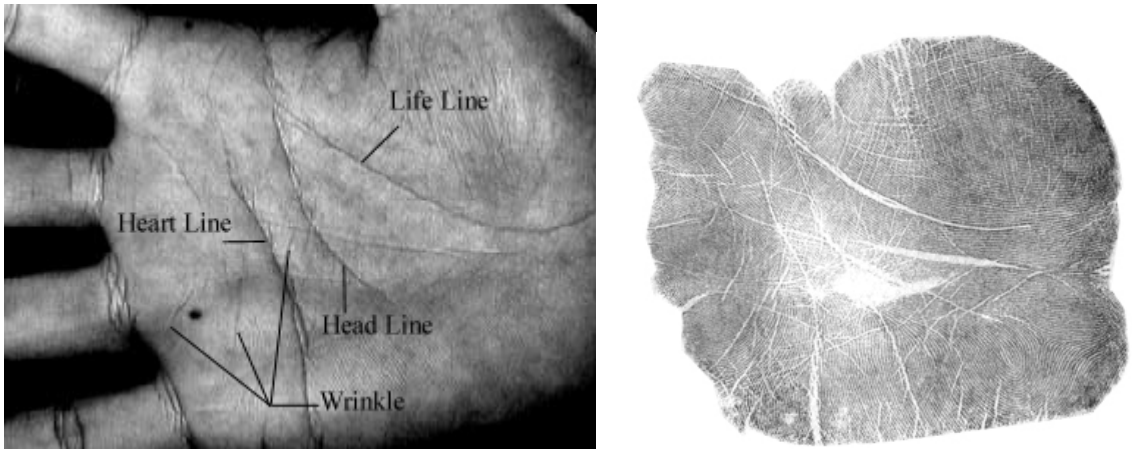

(a) (b)

Fig. 1

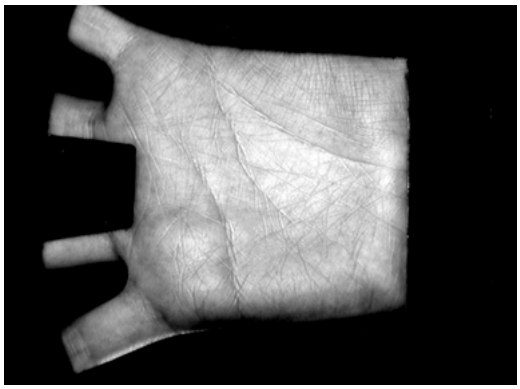

(a)

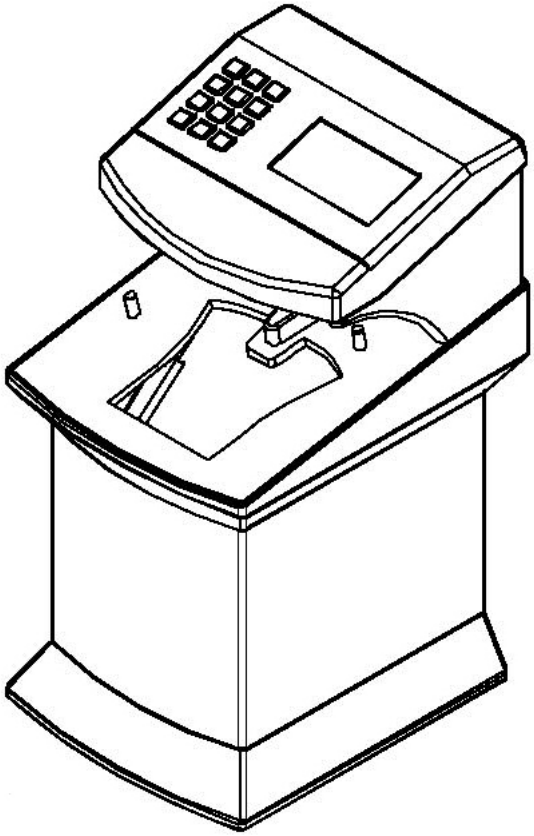

(b)

Fig. 2

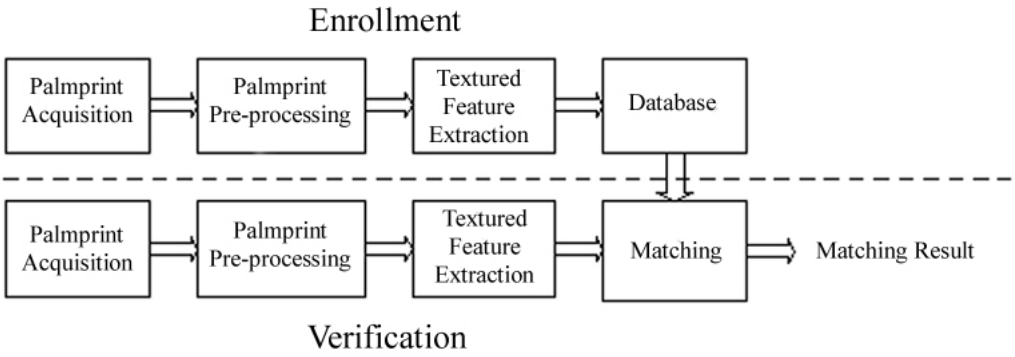
Enrollment
Palmprint Acquisition
Palmprint Pre-processing
Textured Feature Extraction
Database
Palmprint Acquisition
Palmprint Pre-processing
Textured Feature Extraction
Matching
Matching Result
Verification

Fig. 3

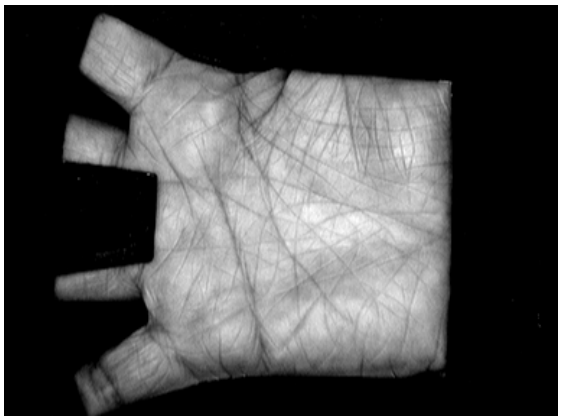

(a)

(b)

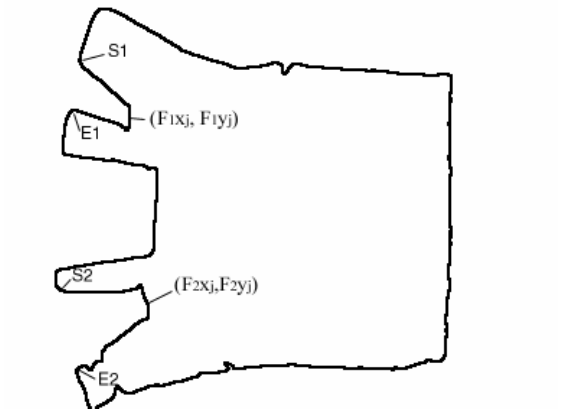

(c)

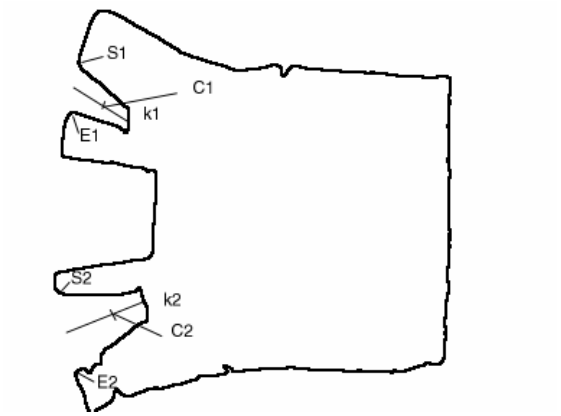

(d)

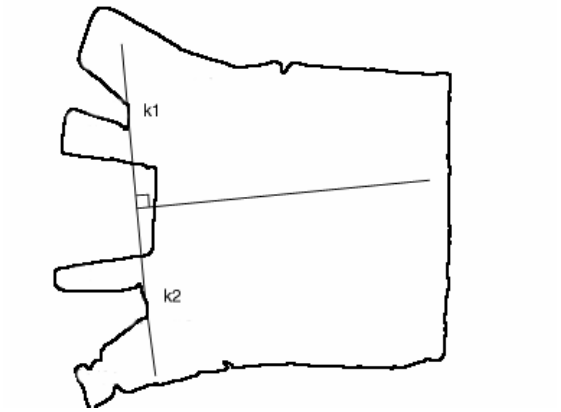

(e)

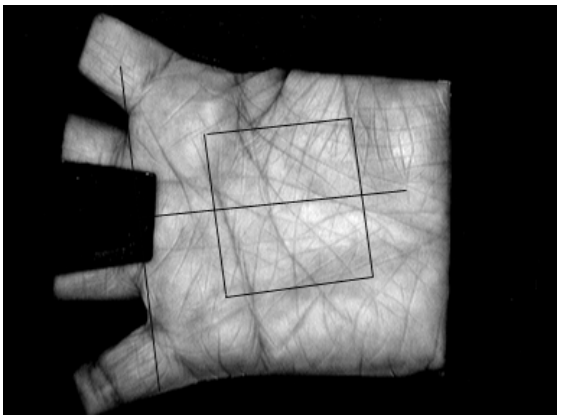

(f)

Fig.4

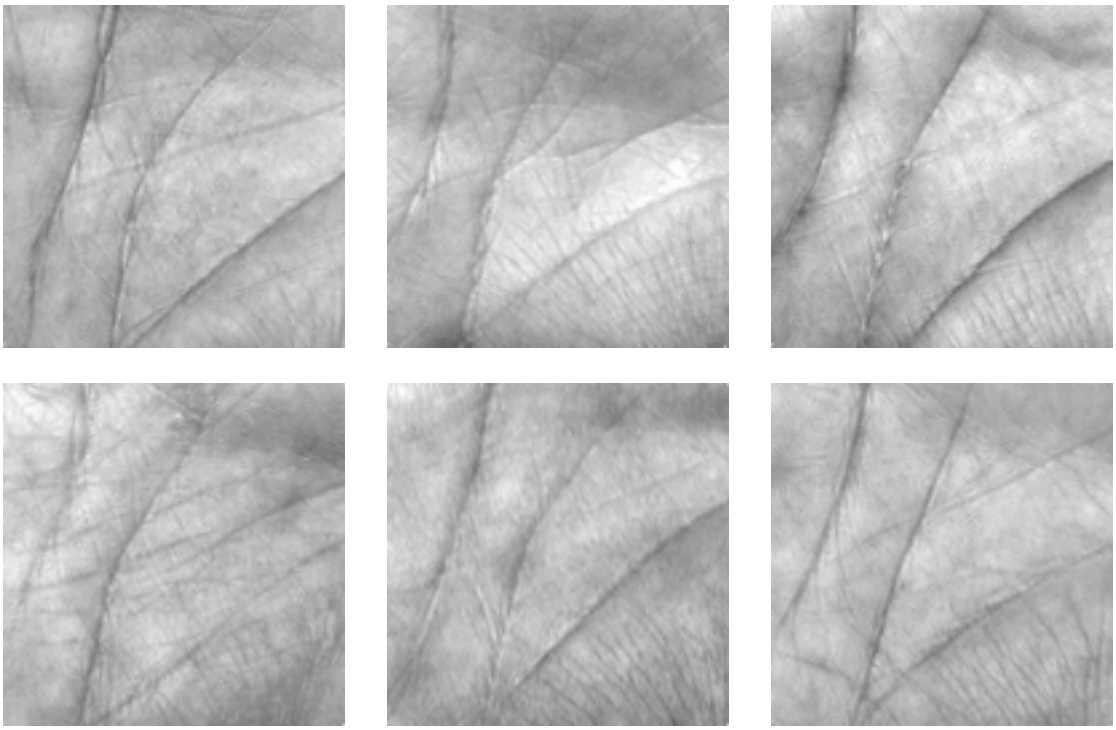

Fig. 5

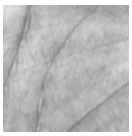

(a)

(b)

(c)

(d)

(e)

(f)

(g)

Fig. 6

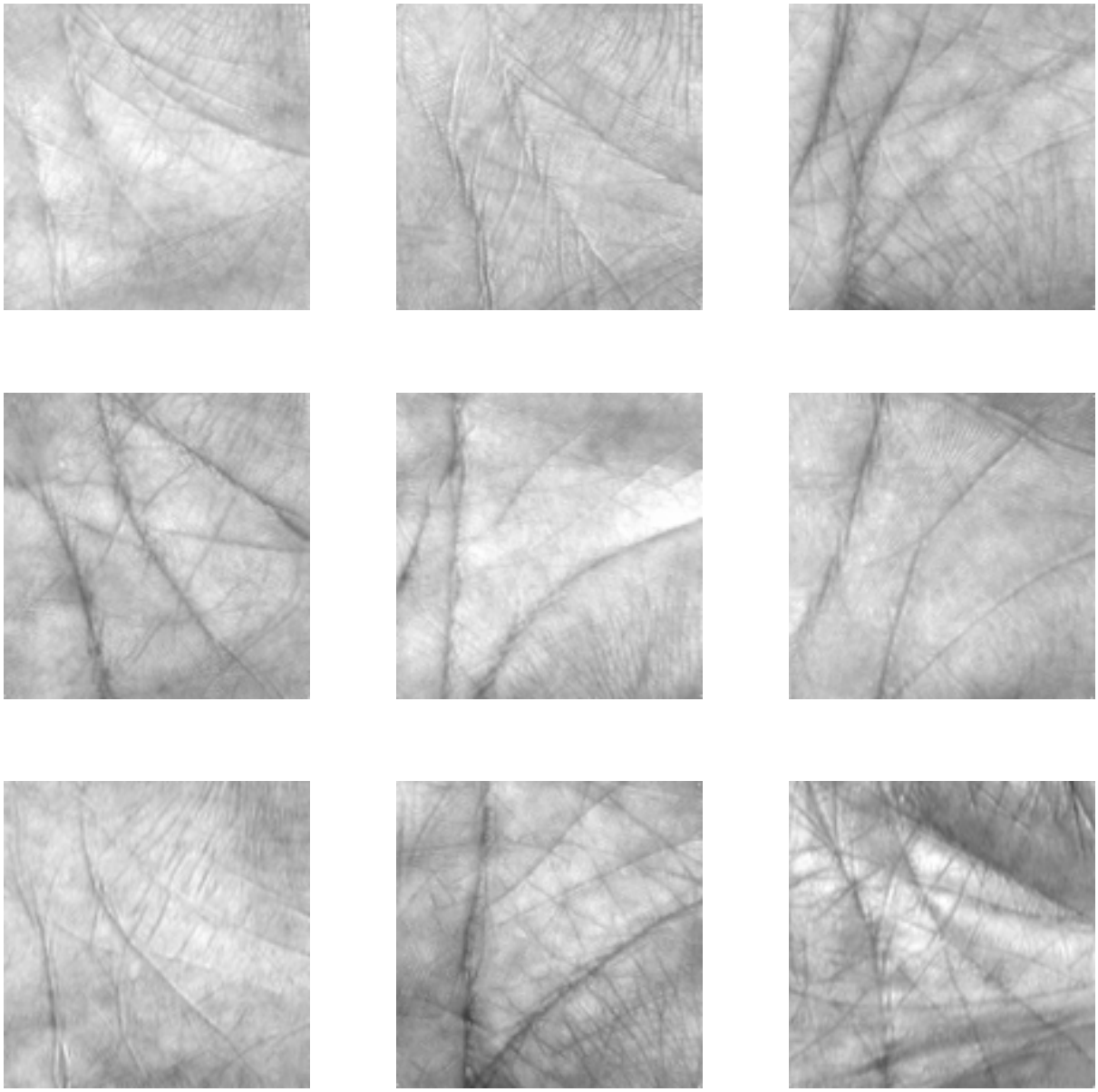

Fig. 7

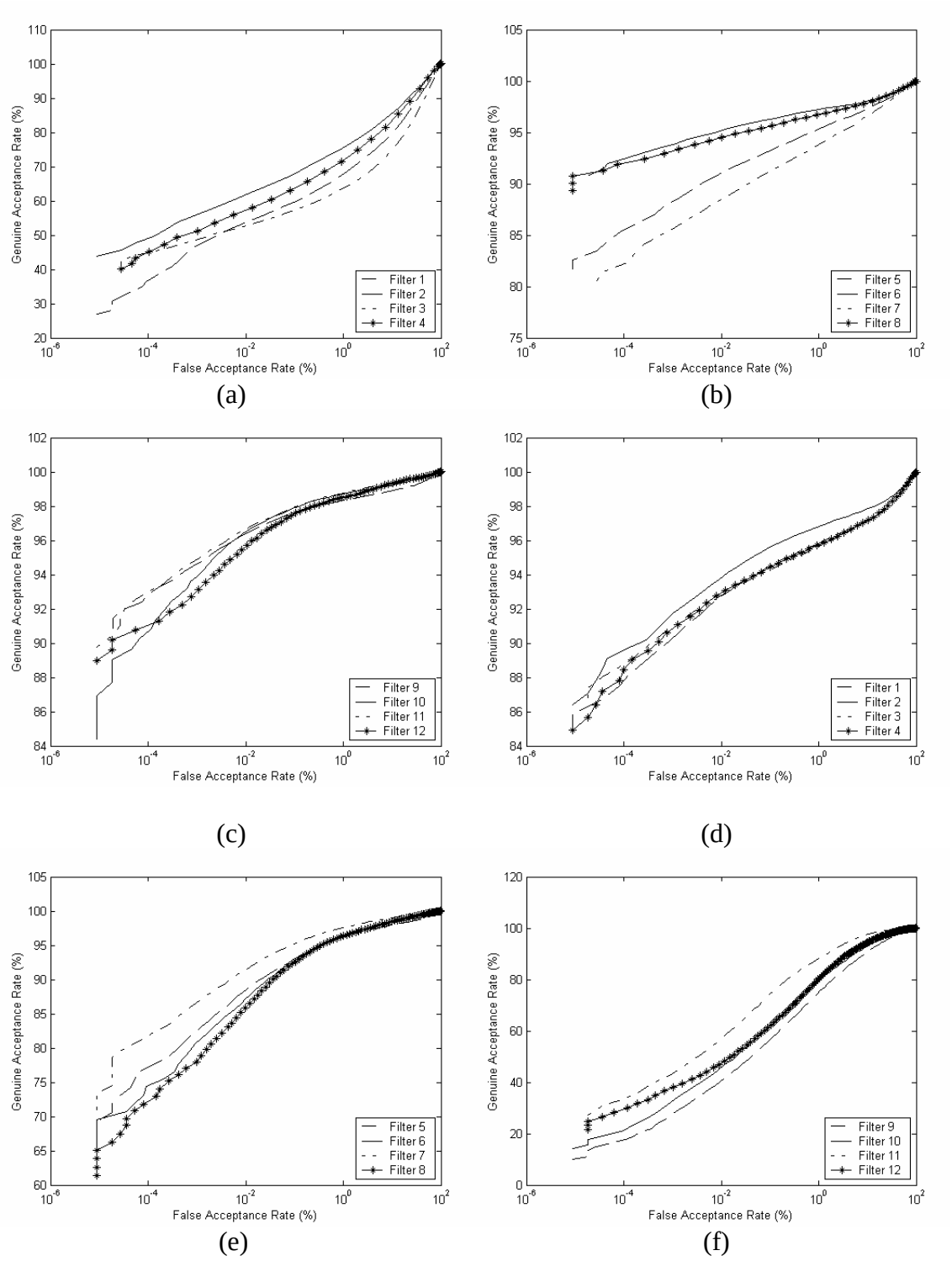
Genuine Acceptance Rate (%)
False Acceptance Rate (%)
Filter 1
Filter 2
Filter 3
Filter 4
(a)
Filter 5
Filter 6
Filter 7
Filter 8
(b)
Filter 9
Filter 10
Filter 11
Filter 12
(c)
Filter 1
Filter 2
Filter 3
Filter 4
(d)
Filter 5
Filter 6
Filter 7
Filter 8
(e)
Filter 9
Filter 10
Filter 11
Filter 12
(f)

Fig. 8

Tables

Table 1

Levels	No	Sizes	q	u	s
1	1	9 by 9	0	0.3666	1.4045
	2	9 by 9	45	0.3666	1.4045
	3	9 by 9	90	0.3666	1.4045
	4	9 by 9	135	0.3666	1.4045
2	5	17 by 17	0	0.1833	2.8090
	6	17 by 17	45	0.1833	2.8090
	7	17 by 17	90	0.1833	2.8090
	8	17 by 17	135	0.1833	2.8090
3	9	35 by 35	0	0.0916	5.6179
	10	35 by 35	45	0.0916	5.6179
	11	35 by 35	90	0.0916	5.6179
	12	35 by 35	135	0.0916	5.6179